Am J Cancer Res 2021;11(11):5402-5414
www.ajcr.us /ISSN:2156-6976/ajcr0135913

Original Article

Genome-wide identification of m6A-associated functional SNPs as potential functional variants for thyroid cancer

Xianhui Ruan[1*], Mengran Tian[1*], Ning Kang[1*], Weike Ma[1], Yu Zeng[1], Gaojian Zhuang[3], Wei Zhang[1], Guangwei Xu[1], Linfei Hu[1], Xiukun Hou[1], Wenjun Xie[6], Ming Gao[1,2], Yongjun Piao[5], Shicheng Guo[4], Xiangqian Zheng[1]

[1]Department of Thyroid and Neck Tumor, Tianjin Medical University Cancer Institute and Hospital, National Clinical Research Center for Cancer, Key Laboratory of Cancer Prevention and Therapy, Tianjin's Clinical Research Center for Cancer, Tianjin 300060, China; [2]Department of Thyroid and Breast Tumor, Tianjin Union Medical Center, Tianjin 300121, China; [3]Department of Thyroid and Breast Tumor, The Sixth Affiliated Hospital of Guangzhou Medical University, Qingyuan People's Hospital, Guangzhou 511500, Guangdong, China; [4]Department of Medical Genetics, School of Medicine and Public Health, University of Wisconsin-Madison, Madison, WI 53726, USA; [5]School of Medicine, Nankai University, Tianjin 300071, China; [6]Department of Basic Surgery, Fujian Provincial Hospital, Fuzhou 350001, Fujian, China. [*]Equal contributors.

Received June 1, 2021; Accepted September 16, 2021; Epub November 15, 2021; Published November 30, 2021

Abstract: m6A methylation has been demonstrated to be one of the most important epigenetic regulation mechanisms in cell differentiation and cancer development especially m6A derived diagnostic and prognostic biomarkers have been identified in the past several years. However, systemic investigation to the interaction between germline single-nucleotide polymorphisms (SNPs) and m6A has not been conducted yet. In this study, we collected previous identified significant thyroid cancer associated SNPs from UKB cohort (358 cases and 407,399 controls) and ICR cohort (3,001 patients and 287,550 controls) and thyroid eQTL (sample size = 574 from GTEx project) and m6A-SNP (N = 1,678,126) were applied to prioritize the candidate SNPs. Finally, five candidate genes (*PLEKHA8, SMUG1, CDC123, RMI2, ACSM5*) were identified to be thyroid cancer associated m6A-related genetic susceptibility. Loss and gain function studies of m6A writer proteins confirm that ACSM5 is regulated by m6A methylation of mRNA. Moreover, ACSM5 is downregulated in thyroid cancer and inversely correlated with PTC malignancy and patient survival. Together, our study highlight mRNA-seq and m6A-seq double analysis provided a novel approach to identify cancer biomarkers and understanding the heterogeneity of human cancers.

Keywords: Epigenetics, m6A, RNA methylation, thyroid cancer, ACSM5

Introduction

Thyroid cancer incidence rate has gradually increased on average, 3.6% annually, r (95% CI, 3.2%-3.9%) from 1974 to 2013, which brings heavy burden to human and society [1]. According to epidemiological investigations, the incidence and mortality rates of advanced-stage papillary thyroid cancer were 3.6% and 1.1% during 1974-2013 [2], suggesting more attention should be paid to early diagnosis and treatment of thyroid carcinoma. The most common histology type is papillary thyroid cancer (PTC) which accounts for 90% of thyroid cases [3]. Most patients with PTC are free of the disease after initial treatment with surgical excision, radioactive iodine and endocrine hormone therapy; nevertheless, approximately 10% of patients die of recurrence and distant metastases within a few years of diagnosis [4]. Over the past decades, the molecular pathogenesis of thyroid cancer has been intensively studied, for instance, variety of mutations in MAPK/ERK pathway and PI3K/AKT pathway factors have been reported in PTC cases, particularly BRAFV600E mutation, and RET/PTC rearrangement [5]. While, the genetic changes during the initiation and progression of PTC are largely

unknown [6]. Therefore, identification of new molecular targets that contribute to early diagnosis and targeted therapy is necessary.

Among hundred types of chemical modifications on cellular RNAs, N6-methyladenosine modification (m6A) is the most abundant modification [7] which usually occurs in the consensus sequence region of RRm6ACH ([G/A/U][G>A]m6AC[U>A>C]); enriched in 3' untranslated region (UTR), the coding region, and near stop codons, particularly [8]. The amount of m6A modification is regulated by the methyltransferase complex (MTC) which include METTL3, METTL14 [9], METTL16 [10], RBM15, VIRMA [11], WTAP [12], and ZC3H13 [13]. The mRNA binding to m6A can be recognized by specific reading proteins that affect the stability, translation and/or localization of the mRNA [14]. Furthermore, eraser protein can remove methylate modification and change the biological function of m6A [15]. Therefore, it's a dynamic and reversible process. In recent years, it has been proved that m6A has a direct effect on many kinds of tumor progression and provide new directions for the treatment of tumors. Due to the m6A methylation modification process is reversible, and with the different modified target genes and different reading proteins, which can lead to different results that promote cancer or suppress cancer. In acute myeloid leukemia (AML) cells, METTL3 expression is more abundant compared with healthy hematopoietic stem/progenitor cells and depletion of METTL3 could delay leukemia [16]. METTL3 is also necessary in EMT of gastric cancer. Elevated METTL3 level could predict poor prognosis of patients [17]. Whereas, the expression of writers were lower in some kind of cancer like endometrial cancer. Reducing the level of m6A modification on mRNA in endometrial cancer cells could promote cell proliferation and tumorigenicity through changing the expression of key enzymes affecting AKT signaling pathway [18]. Besides, downregulation of METTL3 activated p-p38 and p-ERK in colorectal cancer (CRC), which suggested METTL3 plays a tumor suppressor role in CRC [19]. Therefore, more research should be done to understand the mechanisms of m6A modification in tumourigenesis and progression.

As a pivotal enzyme in the first step of fatty acid metabolism, Acyl-coenzyme A synthetase Medium Chain Family Member 5 (ACSM5) could catalyzes the activation of fatty acids by CoA to produce acyl-CoA [20]. Remarkably, it has been reported that SNP in the *ACSM5* promoter region was the most associated polymorphism with the ACSM5 expression levels [21]. However, there are few studies on ACSM5 and only one study has shown that *ACSM5* has been identified as one of eight genetic features that can accurately provide prognostic predictions and new treatments for patients with lung adenocarcinoma (LUAD) [22]. Therefore, the potential roles of ACSM5 in cancer progression and diagnosis need further investigate.

In this study, we aimed at identifying m6A associated functional SNPs of thyroid cancer through integrated database analysis. The results indicate that ACSM5 associated SNPs could prevent m6A modification thus causing mRNA degradation and downregulating its protein level. Additionally, low expression of ACSM5 is associated with aggressive clinicopathological characteristics and poor prognosis. Our study provided a novel approach to identify cancer biomarkers and understanding the new mechanisms of human cancers development.

Results

Genome-wide identification of m6A associated thyroid cancer susceptibility

We firstly collected identified significant thyroid cancer associated SNPs from UK-Biobank cohort (358 cases and 407,399 controls) and ICR cohort (3,001 patients and 287,550 controls) and thyroid eQTL (sample size = 574 from GTEx project) and m6A-SNPs (N = 1,678,126) were applied to prioritize the candidate SNPs. Finally, five candidate genes were identified to be thyroid cancer associated m6A-related genetic susceptibility factors including *PLEKHA8, SMUG1, CDC123, RMI2, ACSM5* (**Figure 1**). Next, we analyzed these candidate genes expression level in pan-cancer samples from TCGA datasets. We observed significant downregulation of ACSM5 in pan-cancer samples (SMD = -2.44, 95% CI: -2.93 to -1.95, TCGA project, **Figure 2**). While, *PLEKHA8, SMUG1, CDC123* and *RMI2* are up-regulated in pan-cancer samples (Supplementary Figure 1).

ACSM5 is regulated by its RNA m6A modification

In order to further identify whether these candidate genes can be regulated by m6A modifica-

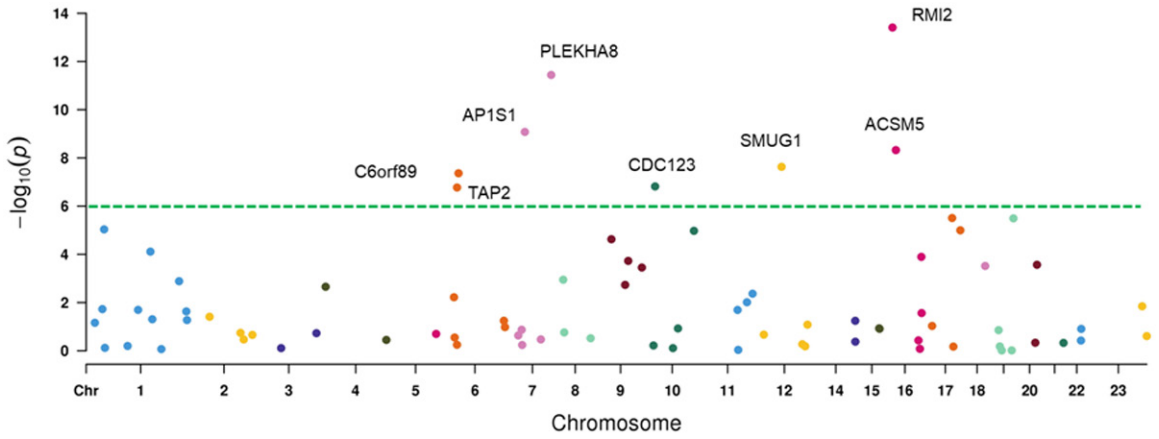

Figure 1. Manhattan plot to show m6A-related significant differential expression thyroid cancer genes (differential expression $P<10^{-6}$ as suggestive significance). GWAS association ($P<0.0001$) are derived from UKB and ICR cohort including *PLEKHA8, SMUG1, CDC123, RMI2, ACSM5* while *TAP2, AP1S1* and *C6orf89* showed significant differential expression, but without significant GWAS signals. Candidate genes are defined as consistent genes with m6A-gain and over-expression as well as m6A-loss and down-regulation in thyroid cancers by GTEx-V8 database.

tion, we then stably knocked down METTL3 in TPC-1 cells and knockdown efficiency was determined by western blot (**Figure 3A**). m6A% content in total RNA detection showed that METTL3 knockdown cells had significantly lower levels of m6A than control cells, which also confirmed the roles of METTL3 as m6A writer of mRNA (**Figure 3B**). We next detected the mRNA level of those candidate genes in these cell lines, strikingly, the results showed that only ACSM5 expression level was significantly downregulated by METTL3 knockdown (**Figure 3C**). We also detected the protein level of ACSM5 in stable cell line, the result showed that ACSM5 was reduced in METTL3 knockdown cells (**Figure 3D**). Consistently, the expression level of ACSM5 was further confirmed decreased by METTL3 inhibition as well as in other thyroid cancer cell lines (Supplementary Figure 2). By applying m6A RNA-immunoprecipitation (RIP) qPCR, we conformed that the m6A level of ACSM5 mRNA was significantly decreased after METTL3 inhibition (**Figure 3E**).

To further confirm above results, we overexpressed METTL3 and METTL14 in KTC-1 cells. Stable cell lines were verified by western blot (**Figure 4A**). We then detected the mRNA level of candidate genes and found the expression of ACSM5 was dramatically upregulated in METTL3 and METTL14 overexpression cells. However, the expression of other candidate genes did not show any significantly change (**Figure 4B**). Consistently with mRNA expression, the protein level of ACSM5 were also upregulated in cells overexpressing METTL3 and METTL14 (**Figure 4C**), and as expected, the m6A level of ACSM5 mRNA were notably increased after the overexpression of METTL3 (**Figure 4D**). Taken together, these data indicated that ACSM5 was regulated by m6A modification writer proteins. In addition, we also predicted the potential m6A modification sites of ACSM5 through the SRAMP (http://www.cuilab.cn/sramp), and then overlapped them with SNP sites of ACSM5 form NCBI. Interestingly, all the very high confidence m6A modification sites contain SNP mutations (Supplementary Figure 3). All together, these data indicated that the expression level of ACSM5 was regulated by m6A modification in thyroid cancer.

ACSM5 expression is down-regulated in thyroid cancer and associated with poor prognosis

To investigate the expression of ACSM5 in thyroid cancer tissues, we compared the expression of ACSM5 between patient PTC and paired normal tissues. As shown in **Figure 5A**, a reduction in ACSM5 transcripts was observed in patient PTC samples compared with paired normal tissues. Analysis of TCGA database showed that, compared with normal tissues, ACSM5 expression levels were much lower in PTC, this result is consistent with our cohort (**Figure 5B**). In addition, ACSM5 expression levels were significantly lower in patients with

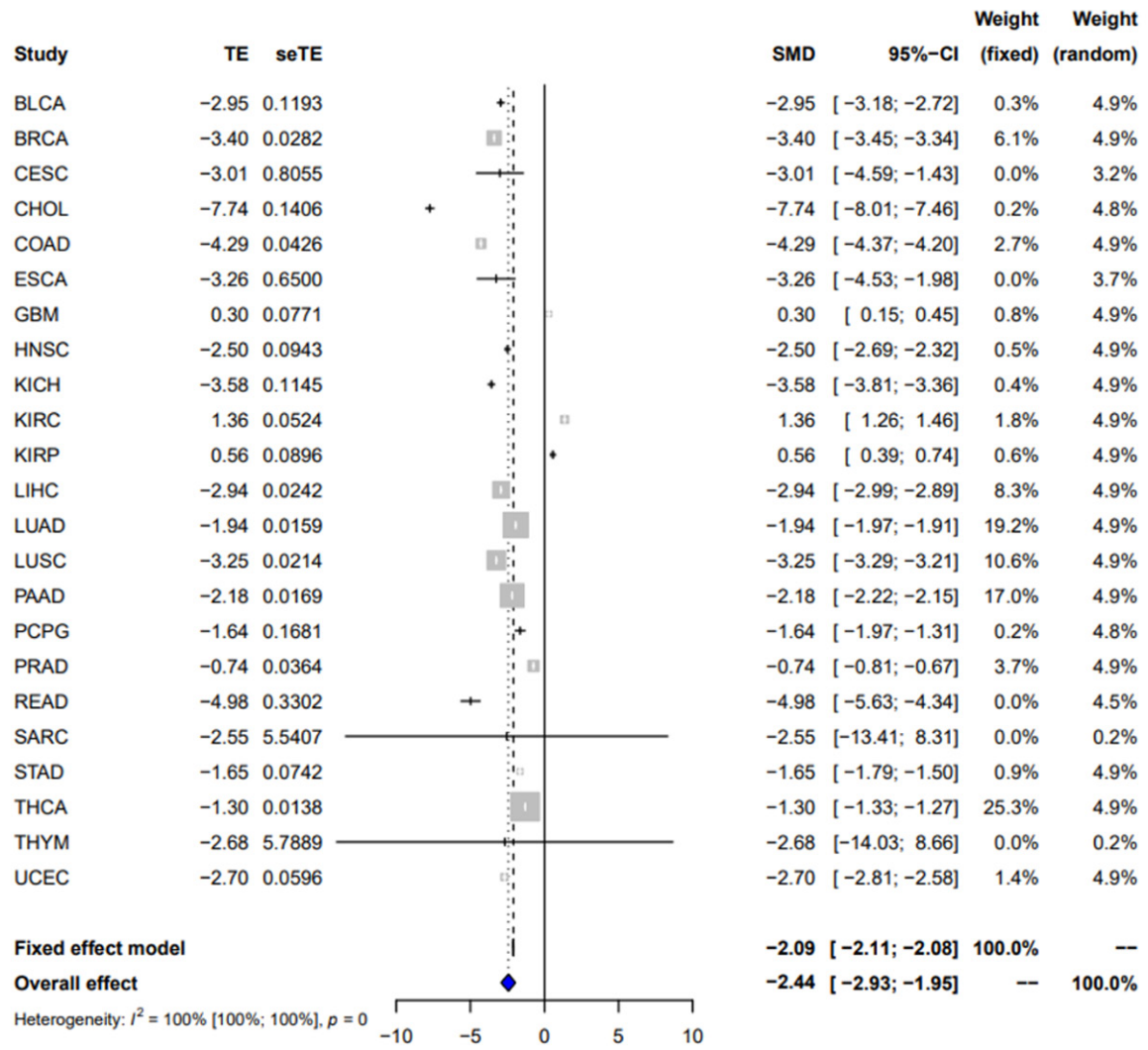

Figure 2. Pan-cancer down-regulation of *ACSM5* crosses 23 types of human cancers. Cancer samples were collected from the TCGA project (N = 10,490). Gene expression level was log2 transformed before the meta-analysis. Both fixed effect model and random effect model were applied for the aggregation. 95% CI was applied to show the risk and protective effect to overall survival time. In order to show more details for different studies, any standardized mean difference (SMD) higher than 3 and lower than -3 was showed with arrow. Blue filled parallelograms represent the SMD for fixed effect model and random effect model.

stage IV than those in patients with stage I/II (**Figure 5C**). Moreover, ACSM5 expression levels were significantly lower in patients with lymph node metastasis (N1 group) than in patients without lymph node metastasis (N0 group). In addition, ACSM5 expression level was negatively correlated with tumor size (**Figure 5C**). Furthermore, we also analyzed the correlation between ACSM5 and METTL3 or METTL14 in TCGA datasets and the results suggested that the expression levels of ACSM5 and METTL3 or METTL14 were positively correlated (**Figure 5D**). Additional efforts were made to explore the prognostic value of ACSM5 in thyroid cancer. ACSM5 low expression was related with poor PFI (P = 0.0036) and OS (P = 0.035) (**Figure 6**). Overall, patients with low ACSM5 expression have an unfavorable prognosis, thus indicating that ACSM5 is a potential prognostic marker for PTC patients.

Discussion

Thyroid cancer is the most common endocrine-related cancer, and its incidence rate has increased rapidly in recent years [23]. There-

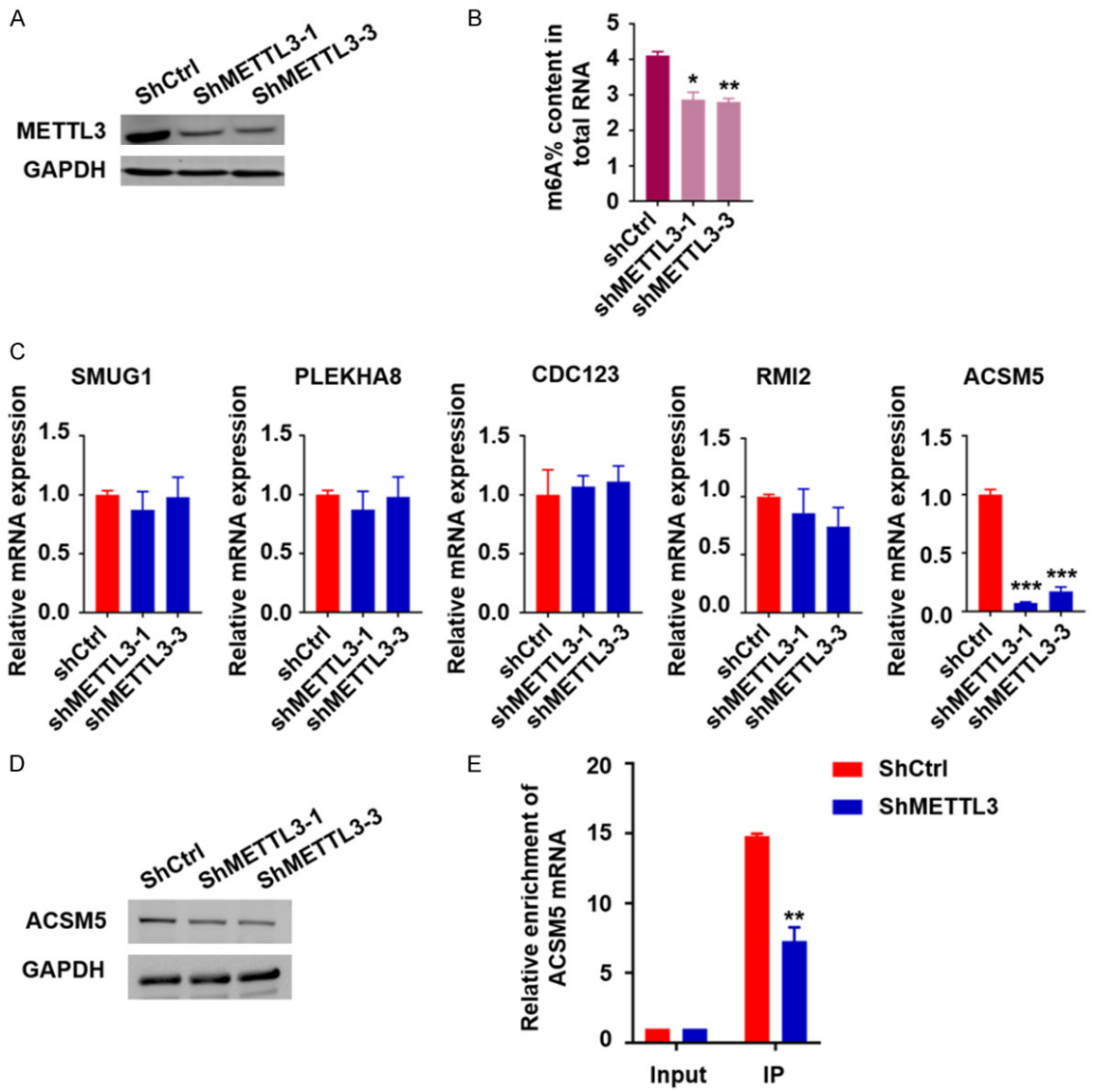

Figure 3. Knockdown *METTL3* inhibits *ACSM5* expression and reduces its RNA m6A modification in thyroid cancer cell. A. *METTL3* level was detected by western blot in *METTL3* stable knock-down TPC-1 cells. B. m6A level was analyzed by ELSIA in TPC-1 cells. C. *SMUG1, PLEKHA8, CDC123, RIM2* and *ACSM5* mRNA in *METTL3* knock-down TPC-1 cells were examined by qRT-PCR. D. Western blot of *ACSM5* level in *METTL3* knock-down TPC-1 cells, GADPH was as the loading control. E. m6A RIP-PCR analysis of *ACSM5* mRNA in the control and *METTL3* knockdown thyroid cancer cells. In all bars, values are shown as mean ± SEM. $^{*}P<0.05$, $^{**}P<0.01$, $^{***}P<0.001$.

fore, exploring the potential biomarkers is of great significance to the diagnosis and treatment of thyroid cancer. Increasing evidence indicated that m6A mRNA modification participates in a number of biological functions including tumorigenesis and progression [24]. However, most studies were focused on the function of m6A modification related proteins in cancer development. To our best knowledge, whether SNP variant can affect mRNA m6A modification thereby changing protein expression to promote cancer progression keeps largely unknown.

In this study, we first identified m6A-associated functional SNPs by combining multiple datasets of thyroid cancer. Further studies demonstrated that one candidate gene *ACSM5* was down-regulated after METTL3 knockdown, which indicating the low-expression of ACSM5

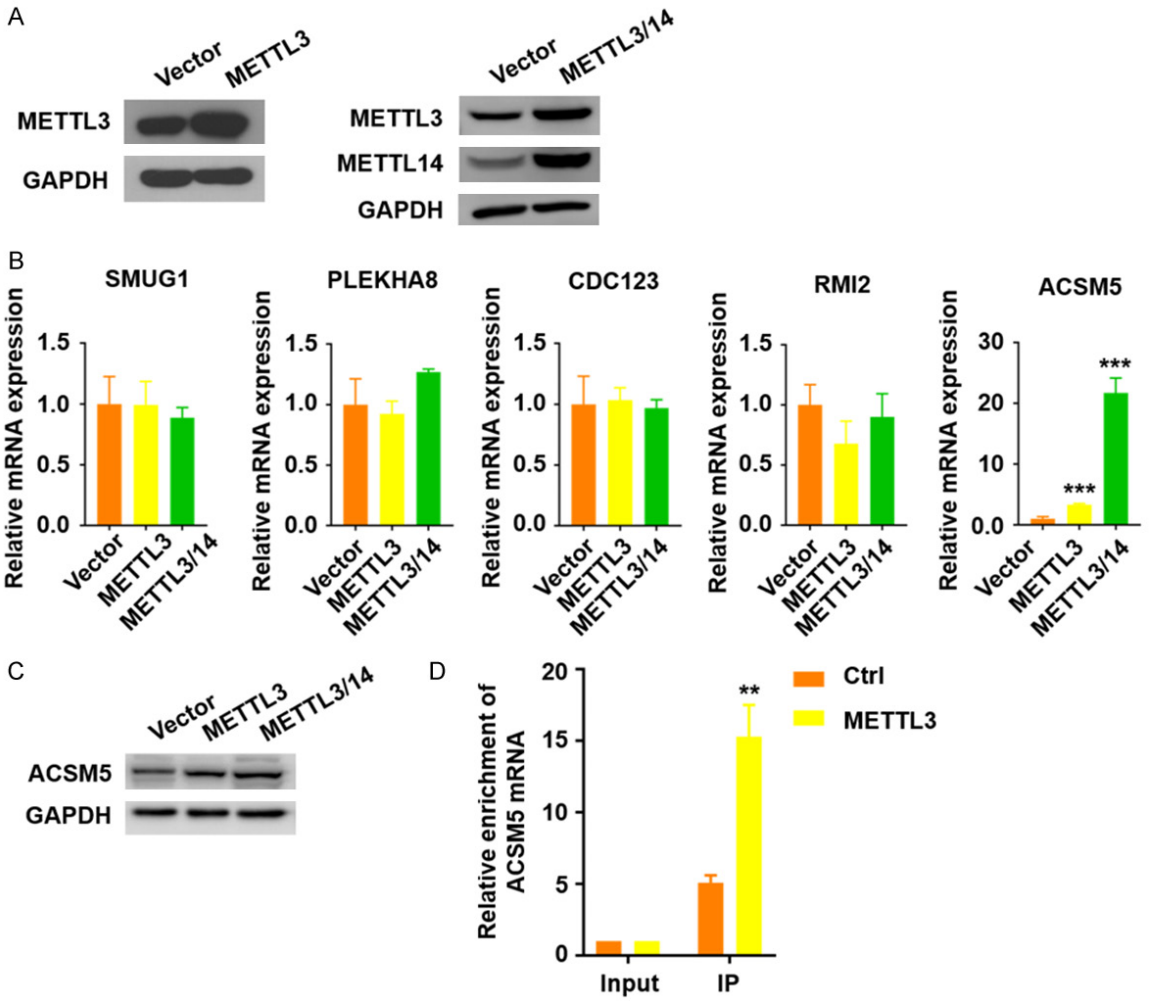

Figure 4. Overexpression *METTL3* and *METTL14* upregulate *ACSM5* expression in thyroid cancer. A. *METTL3* or *METTL14* level was detected by western blot in *METTL3* or *METTL14* overexpression KTC-1 cells. B. SMUG1, PLEKHA8, CDC123, RIM2 and *ACSM5* mRNA in *METTL3* or *METTL14* overexpression KTC-1 cells were examined by qRT-PCR. C. *ACSM5* protein level was detected in *METTL3* or *METTL14* overexpression KTC-1 cells, GAPDH was as the loading control. D. m6A RIP-PCR analysis of ACSM5 mRNA in the control and METTL3 overexpression thyroid cancer cells. In all bars, values are shown as mean ± SEM. $^{*}P<0.05$, $^{**}P<0.01$, $^{***}P<0.001$.

might be caused by RNA methylation loss caused non-stability. We then checked the ACSM5 expression level in thyroid cancer tissues and paired normal tissues and found its expression level was significant down-regulated, indicating *ACSM5* might be a tumor suppresser gene. The TCGA database analysis further confirmed that low ACSM5 expression in thyroid cancer was associated with aggressive clinicopathological features. To the best of our knowledge, ACSM5, which is involved in the first step of fatty acid metabolism, that is, CoA catalyzes the activation of fatty acids to produce acyl CoA, was rarely investigated in tumors. In a recent study, Ma *et al.* reported that an eight-gene signature including *ACSM5* could accurately identify patients' prognosis, suggesting ACSM5 may play a role in lung cancer progression [22]. The role of ACSM5 in tumor progression, especially in thyroid cancer, is still largely unknown and warrants further exploration.

Meanwhile, we also observed that ACSM5 expression level was positive correlated with METTL3 or METTL14 expression level in TCGA datasets, which supporting ACSM5 might be regulated by m6A modification. METTL3 and METTL14, which are the methyltransferase of mRNA m6A modification, exhibits various roles

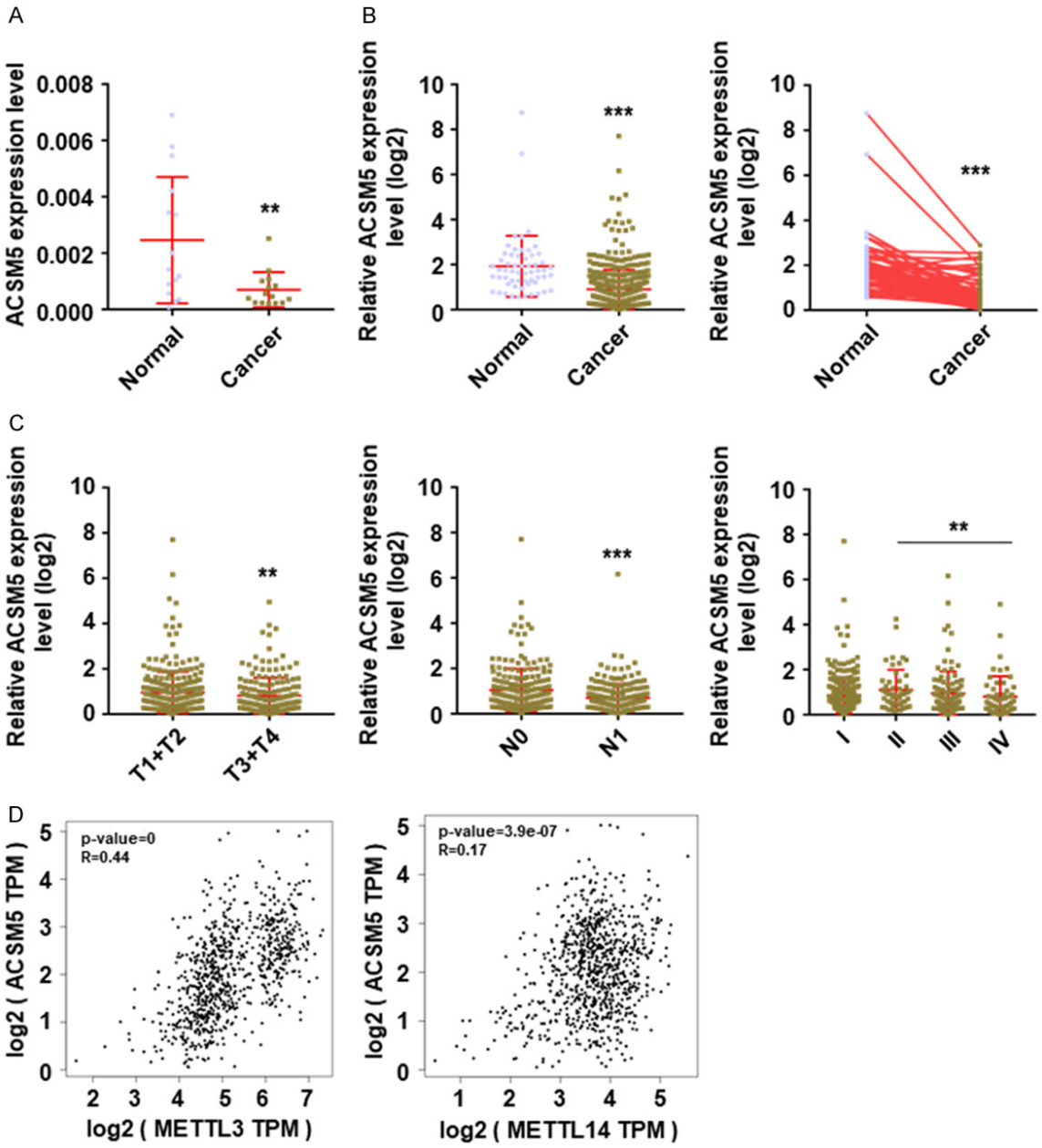

Figure 5. *ACSM5* is downregulated in PTC specimens and associated with cancer progression. A. *ACSM5* mRNA levels in PTC samples and matched normal thyroid tissues (MN) were analyzed by qRT-PCR (n = 16). B. *ACSM5* expression levels in PTCs (n = 504) and normal thyroid tissues (NT) (n = 59) or PTC samples and matched normal thyroid tissues (MN) (n = 59) in TCGA dataset. C. *ACSM5* expression levels of different T stage, N stage and TNM stage in PTCs, data were obtained from TCGA dataset. D. Relationship between *ACSM5* expression levels and *METTL3* or *METTL14* expression levels in PTCs. $^{*}P<0.05$, $^{**}P<0.01$, $^{***}P<0.001$.

in cancer cells, such as: contributing myeloid leukemia [25], promoting liver cancer progression [26], playing important roles in GSC maintenance and radio-resistance [27], positively regulating proliferation of hematopoietic stem/progenitor cells (HSPCs) [16], and triggering the translation in cancer cells [28]. However, their functions in thyroid cancer development are still unclear. Wang *et al.* reported that METTL3 was upregulated in thyroid cancer and promoted thyroid cancer progression by m6A methylation on TCF1 [29]. While, our preliminary study demonstrated that METTL3 was downregulated in thyroid cancer of our cohort

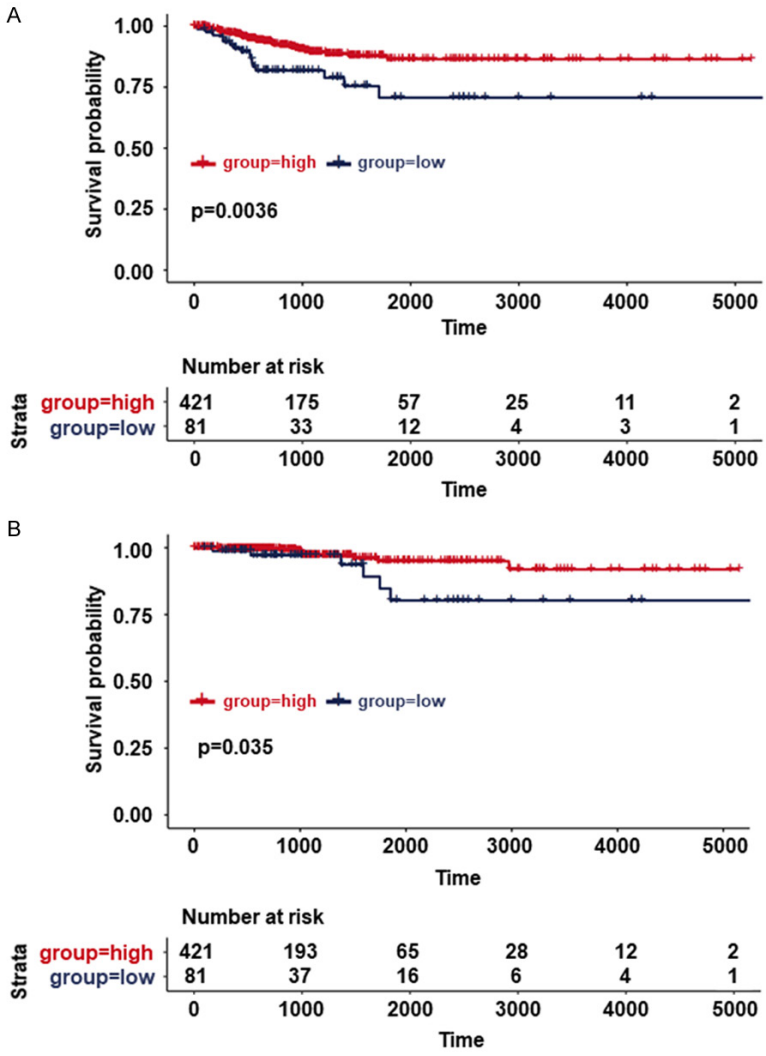

Figure 6. The prognostic value of *ACSM5* expression for papillary thyroid cancer patients. Low expression of *ACSM5* in PTCs was related with poor PFI (A) and OS (B), Data were obtained from TCGA database.

and inhibited thyroid cancer development (data not shown). This may be due to METTL3 has a variety of roles as opposed to singularly being a tumor suppressor or promoter in thyroid carcinogenesis. According to our study, METTL3 may inhibit the progression of thyroid cancer by increasing the methylation level of ACSM5. Another previous study performed a comprehensive evaluation of the m6A RNA modification landscape of PTC to build a m6A-related signature which was capable to predict the DFS of patients and acted as an independent prognostic factor for PTC [30]. All these studies indicate that mRNA m6A modification plays important roles in thyroid cancer development, but its underlying mechanisms warrant further study.

In thyroid cancer, several GWASs had been performed in different populations. Some single-nucleotide polymorphisms (SNPs) associated with susceptibility to thyroid cancer were identified in previous studies, including markers near FOXE1, NKX2-1, DIRCS, NRG1, IMMP, FOXA2, DIR3 and so on. Among these, only several SNPs were confirmed in different populations by targeted genotyping methods [31-34]. Therefore, more SNPs associated with thyroid cancer should be identified in the further study. In this study, we performed meta-analysis, thyroid eQTL and m6A-SNP analysis to discover new candidate SNPs in thyroid cancer and found several novel susceptibility loci (PLEKHA8, SMUG1, CDC123, RMI2 and ACSM5) may be associated with thyroid cancer. The eQTL analysis suggested that ACSM5-SNPs were the negative eQTL, indicating low expression of ACSM5 was a high risk factor for thyroid cancer. Moreover, pan-cancer analysis showed that ACSM5 was downregulated in most cancer types including thyroid cancer. While, more large-scale GWAS studies of different populations are needed to confirm these novel susceptibility loci.

The limitation of this study is that we only tested mRNA level of ACSM5 in thyroid cancer tissues, and a further immunohistochemistry experiment is needed to evaluate the expression of ACSM5 at the protein level. Another limitation is that we did not demonstrate the candidate SNPs of ACSM5 could affect its RNA methylation as well as protein expression. Of note, the function of ACSM5 in thyroid cancer progression also should be further studied. Lastly, we did not investigate the association between candidate SNPs and clinical phenotypes of papillary thyroid cancer, such as the

BRAFV600E mutation, lymph node metastasis or extrathyroidal extension. The highlight of this study is that this is the first study to reveal that thyroid cancer related SNPs may promote tumor progression by affecting its mRNA m6A modification to change protein expression. In addition, we first report ACSM5 is downregulated in thyroid cancer and could be as a potential biomarker for papillary thyroid cancer.

In conclusion, we conducted a new bioinformatic analysis method to predict the new SNPs in thyroid cancer. We revealed novel susceptibility loci at ACSM5. We also validated these SNPs might downregulate ACSM5 protein level by affecting its m6A modification. More importantly, low expression of ACSM5 is associated poor prognosis of thyroid cancer. We hope that the results of this study will provide insights into the diagnosis and treatment of thyroid cancer in the future, and provide more insights into genetic factors in the era of personalized cancer treatment.

Materials and methods

Identification of m6A-SNP and derived differential expression in pan-cancer RNA-seq dataset

m6A-SNPs are defined as the SNPs which would change the motif of specific genomic-short-region, therefore, m6A-modifier protein (METTL3, WTAP, FTO, YTHDC1 etc.) would lose or receive writing, removing or reading ability and finally the expression pattern would be mis-regulated. We collected all m6A-SNP from m6Avar database [35], thyroid cancer associated SNPs from two GWAS studies from UK-Biobank project [36] and Icelandic Cancer Registry (ICR) project [37] (Supplementary Table 1). We merged all the significant thyroid cancer associated SNPs from UKB and ICR project, then intersected with m6A-SNPs derived from m6Avar to identify m6A-mediated thyroid cancer associated risk/protective genes. In order to identify all potential m6A mis-regulated gene expression in human cancers, we downloaded 11,093 gene expression quantification data derived from RNA-seq data from the TCGA database (https://portal.gdc.cancer.gov/repository) on February 24, 2019. The RNA-seq data included 32 cancer types and we removed 9 cancer types owing to low sample size for control samples (N≤1). Log2-transformed fragments per kilobase of transcript per million mapped reads upper quartile (FPKM-UQ) derived from HTSeq [38] was applied for differential gene expression analysis. Bayesian generalized linear model (bayesglm) from ARM package (v1.10-1) was used for differential gene expression analysis. Metafor package (v2.1-0) was applied for meta-analysis across the 23 cancer types. Kaplan-Meier survival analysis was performed to estimate overall survival of low-ACSM5 and high-ACSM5 expression group.

Clinical samples

Thyroid cancer tissue and paired non-cancer tissue samples were collected from patients (n = 16) who underwent surgical resection at the Tianjin Medical University Cancer Institute and Hospital. The detailed clinical pathological characteristics of the thyroid cancer patients are shown in Supplementary Table 2. Samples for quantitative reverse transcription PCR (qRT-PCR) were snap frozen in liquid nitrogen immediately after surgeries and kept at -80°C until usage. Informed consent was obtained from all patients. This study was approved by the Ethics Committee of the Tianjin Medical University Cancer Institute and Hospital.

Cell culture and stable cell line establishment

KTC-1, TPC-1, BCPAP, CAL-62 and HEK293T were all acquired from American Type Culture Collection. All cell lines were identified by short tandem repeat (STR) analysis before using in the experiments. KTC-1, TPC-1, BCPAP and CAL-62 were cultured in RPMI 1640 (Gibco) supplemented with 10% FBS (Biological Industries) and penicillin/streptomycin (5000 units/mL; Gibco). HEK293T was cultured in DMEM medium (Gibco) supplemented with 10% FBS (Biological Industries) and penicillin/streptomycin (5000 units/mL; Gibco). Cells were cultured in a humidified incubator (Thermo Fish Scientific) equilibrated with 5% CO_2 at 37°C. The passage number of the cells used for the experiments was about 20-30. All cells used in the experiment are guaranteed to be negative for mycoplasma detecting.

Cells were infected by lentiviral particles carrying shRNA plasmids for generating stable METTL3 knockdown cell line (shMETTL3-1: GGAACATTATGATCCAGAAAC, shMETTL3-3: GG-

AACTGGATCCTACCTATGT) or control (shGFP). Similarly, stable METTL3 and METTL14 overexpression cell lines were generated by transduction with lentiviral particles containing METTL3, METTL14 or GFP cDNA. Cells were then cultured with complete culture solution with puromycin for 7-10 days after 48 hours lentiviral infection. Recombinant lentiviral particles enriched in medium supernatant were produced by co-transfection of the above vectors and packing plasmids in HEK293T and harvested after centrifuge and filtering to remove cell debris.

Real-time quantitative RT-PCR

Total RNA was extracted from thyroid cancer cells and tissues using RNeasy Mini kit (Qiagen). RNA reverse transcription and Real-time quantitative PCR were performed in strict accordance with the manufacturer's instructions. cDNA synthesis was conducted using Transcriptor First Strand cDNA Synthesis kit (Takara). PCR reactions were performed with FastStart Universal SYBR Green Master (Takara) in a ABI ViiA7 system. PCR cycling conditions were as follows: firstly at 95°C for 10 min, and then proceed with 40 cycles of 95°C for 15 s, 58°C for 15 s, and lastly at 72°C for 30 s, and then a melting curve of the amplified DNA was acquired. Quantification of target genes was normalized with ACTIN. Primers are summarized in Supplementary Table 3.

Antibodies and western blotting

Cance cells were lysed with RIPA lysis buffer (Solarbio) and obtained protein through ultracentrifugation, then BCA Protein Assay kit was used for determation of protein concentration (Solarbio). Protein lysates were separated by 10% SDS-PAGE electrophoresis and target proteins were detected by western blotting with following antibodies: anti-ACSM5 (Thermo Fisher Scientific), anti-METTL3 (Abcam), anti-METTL14 (Abcam), anti-GAPDH (CST).

m6A RNA methylation quantification

RNA (m6A) methylation quantification was performed according to the protocol of m6A RNA Methylation Assay Kit (ab185912). Briefly, 200 ng RNA samples were added into the specific wells, and gently tilt the plate from side to side or shake the plate several times to mix the RNA-binding solution. Ensure the solution coats the bottom of the well evenly. After covering strip plate with plate and incubate at 37°C for 90 min, remove the binding solution from each well and wash every well three times. 50 μL of diluted capture antibody was added to each well and incubated for 60 minutes at room temperature. The diluted detection antibody solution was then removed from each well and the wells were washed five times with wash buffer. The absorbance was measured at 450 nm within 2 to 10 minutes by a microplate reader.

m6A RT-PCR

The m6A-RT-PCR was performed according to the previously described protocol, with slight modifications [39]. From this, 50 ng of total RNA was taken as input and 100 μg of RNA was added to 500 μL of IP buffer (150 mM NaCl, 0.1% NP-40, 10 mM Tris, pH 7.4, 100 U RNase inhibitor) with m6A antibody (ab190-886) and Dyna beads® Protein A (Thermo Fisher Scientific) for immunoprecipitation to obtain the pull-down fraction of m6A (m6A IP fraction), and another 100 μg of RNA was co-incubated with IgG antibody as the non-specifically bound fraction. After gentle rotation overnight in 4 degree, the RNAs were eluted twice with the elution buffer (5 mM Tris-HCL pH 7.5, 1 mM EDTA pH 8.0, 0.05% SDS, 20 mg/ml Proteinase K) and the IP RNAs were recovered by re-precipitation with Trizo and ethanol. The RNAs were reversed separately. It was then used as a template for qRT-PCR as described above. The housekeeping gene HPRT1 was chosen as an internal control, as it was reported that HPRT1 mRNA did not have any m6A peak in the m6A analysis database [40].

Statistical analysis

Statistical analyses were performed using the SPSS 12.0 Statistical Software. Differences between groups were analyzed by unpaired Student's t-test and nonparametric Mann-Whitney test, as well as Chi-Squared Test. All results are showed as mean ± SEM and statistical differences were represented by *P* values in figures ($^{***}P<0.001$, $^{**}P<0.01$, $P<0.05$). $P<0.05$ was considered to be statistically significant. High-throughput differential gene ex-

pression and meta-analysis were conducted under R (v3.6.1).

Acknowledgements

We would like to appreciate Tianjin Medical University Cancer Hospital for the equipment provided by the experimental platform and the experimental technicians involved in this study. We are grateful to the patients who agreed to contribute samples. Moreover, we would like to thank the funders supporting this research. This work was partially supported by grants from National Natural Science Foundation of China (Grant Nos. 81872169), Tianjin key research and development program science and technology support key projects (Grant No. 17YFZCSY00690), Tianjin Municipal Science and technology project (Grant No. 19JCYBJC27400) and Beijing-Tianjin-Hebei Basic Research Cooperation Project (Grant No. 20JCZXJC00120), Youth Scientific Research Project of Fujian Health Commission (Grant No. 2020QNA007), Tianjin Research Innovation Project for Postgraduate Students (Grant No. 2020YJSS181), Introduced Talents and Doctoral Start-up Foundation of Tianjin Medical University Cancer Institute and Hospital (Grant No. B2009).

Disclosure of conflict of interest

None.

Address correspondence to: Dr. Shicheng Guo, Department of Medical Genetics, School of Medicine and Public Health, University of Wisconsin-Madison, Madison, WI 53706, USA. Tel: 281-685-5882; E-mail: Shicheng.Guo@wisc.edu; Dr. Xiangqian Zheng, Department of Thyroid and Neck Tumor, Tianjin Medical University Cancer Institute and Hospital, National Clinical Research Center for Cancer, Key Laboratory of Cancer Prevention and Therapy, Tianjin's Clinical Research Center for Cancer, Tianjin 300060, China. Tel: +86-22-2334-0123 Ext. 3150; E-mail: xzheng05@tmu.edu.cn

References

[1] Cabanillas ME, McFadden DG and Durante C. Thyroid cancer. Lancet 2016; 388: 2783-2795.

[2] Lim H, Devesa SS, Sosa JA, Check D and Kitahara CM. Trends in thyroid cancer incidence and mortality in the United States, 1974-2013. JAMA 2017; 317: 1338-1348.

[3] Raue F and Frank-Raue K. Thyroid cancer: risk-stratified management and individualized therapy. Clin Cancer Res 2016; 22: 5012-5021.

[4] Dong W, Horiuchi K, Tokumitsu H, Sakamoto A, Noguchi E, Ueda Y and Okamoto T. Time-varying pattern of mortality and recurrence from papillary thyroid cancer: lessons from a long-term follow-up. Thyroid 2019; 29: 802-808.

[5] Fagin JA and Wells SA Jr. Biologic and clinical perspectives on thyroid cancer. N Engl J Med 2016; 375: 1054-1067.

[6] Pozdeyev N, Gay LM, Sokol ES, Hartmaier R, Deaver KE, Davis S, French JD, Borre PV, LaBarbera DV, Tan AC, Schweppe RE, Fishbein L, Ross JS, Haugen BR and Bowles DW. Genetic analysis of 779 advanced differentiated and anaplastic thyroid cancers. Clin Cancer Res 2018; 24: 3059-3068.

[7] Roundtree IA, Evans ME, Pan T and He C. Dynamic RNA modifications in gene expression regulation. Cell 2017; 169: 1187-1200.

[8] Zhao BS, Roundtree IA and He C. Post-transcriptional gene regulation by mRNA modifications. Nat Rev Mol Cell Biol 2017; 18: 31-42.

[9] Wang P, Doxtader KA and Nam Y. Structural basis for cooperative function of Mettl3 and Mettl14 methyltransferases. Mol Cell 2016; 63: 306-317.

[10] Warda AS, Kretschmer J, Hackert P, Lenz C, Urlaub H, Höbartner C, Sloan KE and Bohnsack MT. Human METTL16 is a N(6)-methyladenosine (m(6)A) methyltransferase that targets pre-mRNAs and various non-coding RNAs. EMBO Rep 2017; 18: 2004-2014.

[11] Patil DP, Chen CK, Pickering BF, Chow A, Jackson C, Guttman M and Jaffrey SR. m(6)A RNA methylation promotes XIST-mediated transcriptional repression. Nature 2016; 537: 369-373.

[12] Bansal H, Yihua Q, Iyer SP, Ganapathy S, Proia DA, Penalva LO, Uren PJ, Suresh U, Carew JS, Karnad AB, Weitman S, Tomlinson GE, Rao MK, Kornblau SM and Bansal S. WTAP is a novel oncogenic protein in acute myeloid leukemia. Leukemia 2014; 28: 1171-1174.

[13] Knuckles P, Lence T, Haussmann IU, Jacob D, Kreim N, Carl SH, Masiello I, Hares T, Villaseñor R, Hess D, Andrade-Navarro MA, Biggiogera M, Helm M, Soller M, Bühler M and Roignant JY. Zc3h13/Flacc is required for adenosine methylation by bridging the mRNA-binding factor Rbm15/Spenito to the m(6)A machinery component Wtap/Fl(2)d. Genes Dev 2018; 32: 415-429.

[14] Zaccara S, Ries RJ and Jaffrey SR. Reading, writing and erasing mRNA methylation. Nat Rev Mol Cell Biol 2019; 20: 608-624.

[15] Jia G, Fu Y, Zhao X, Dai Q, Zheng G, Yang Y, Yi C, Lindahl T, Pan T, Yang YG and He C. N6-methyl-

adenosine in nuclear RNA is a major substrate of the obesity-associated FTO. Nat Chem Biol 2011; 7: 885-887.
[16] Vu LP, Pickering BF, Cheng Y, Zaccara S, Nguyen D, Minuesa G, Chou T, Chow A, Saletore Y, MacKay M, Schulman J, Famulare C, Patel M, Klimek VM, Garrett-Bakelman FE, Melnick A, Carroll M, Mason CE, Jaffrey SR and Kharas MG. The N(6)-methyladenosine (m(6)A)-forming enzyme METTL3 controls myeloid differentiation of normal hematopoietic and leukemia cells. Nat Med 2017; 23: 1369-1376.
[17] Yue B, Song C, Yang L, Cui R, Cheng X, Zhang Z and Zhao G. METTL3-mediated N6-methyladenosine modification is critical for epithelial-mesenchymal transition and metastasis of gastric cancer. Mol Cancer 2019; 18: 142.
[18] Liu J, Eckert MA, Harada BT, Liu SM, Lu Z, Yu K, Tienda SM, Chryplewicz A, Zhu AC, Yang Y, Huang JT, Chen SM, Xu ZG, Leng XH, Yu XC, Cao J, Zhang Z, Liu J, Lengyel E and He C. m(6)A mRNA methylation regulates AKT activity to promote the proliferation and tumorigenicity of endometrial cancer. Nat Cell Biol 2018; 20: 1074-1083.
[19] Deng R, Cheng Y, Ye S, Zhang J, Huang R, Li P, Liu H, Deng Q, Wu X, Lan P and Deng Y. m(6)A methyltransferase METTL3 suppresses colorectal cancer proliferation and migration through p38/ERK pathways. Onco Targets Ther 2019; 12: 4391-4402.
[20] Luo ZH, Liu ZW, Mao Y, Shu R, Fu LC, Yang RY, Hu YJ and Shen XL. Cajanolactone A, a stilbenoid from cajanus cajan, prevents ovariectomy-induced obesity and liver steatosis in mice fed a regular diet. Phytomedicine 2020; 78: 153290.
[21] Revilla M, Puig-Oliveras A, Crespo-Piazuelo D, Criado-Mesas L, Castelló A, Fernández AI, Ballester M and Folch JM. Expression analysis of candidate genes for fatty acid composition in adipose tissue and identification of regulatory regions. Sci Rep 2018; 8: 2045.
[22] Ma C, Luo H, Cao J, Zheng X, Zhang J, Zhang Y and Fu Z. Identification of a novel tumor microenvironment-associated eight-gene signature for prognosis prediction in lung adenocarcinoma. Front Mol Biosci 2020; 7: 571641.
[23] Kim J, Gosnell JE and Roman SA. Geographic influences in the global rise of thyroid cancer. Nat Rev Endocrinol 2020; 16: 17-29.
[24] Huang H, Weng H and Chen J. m(6)A modification in coding and non-coding rnas: roles and therapeutic implications in cancer. Cancer Cell 2020; 37: 270-288.
[25] Barbieri I, Tzelepis K, Pandolfini L, Shi J, Millán-Zambrano G, Robson SC, Aspris D, Migliori V, Bannister AJ, Han N, De Braekeleer E, Ponstingl H, Hendrick A, Vakoc CR, Vassiliou GS and Kouzarides T. Promoter-bound METTL3 maintains myeloid leukaemia by m(6)A-dependent translation control. Nature 2017; 552: 126-131.
[26] Chen M, Wei L, Law CT, Tsang FH, Shen J, Cheng CL, Tsang LH, Ho DW, Chiu DK, Lee JM, Wong CC, Ng IO and Wong CM. RNA N6-methyladenosine methyltransferase-like 3 promotes liver cancer progression through YTHDF2-dependent posttranscriptional silencing of SOCS2. Hepatology 2018; 67: 2254-2270.
[27] Visvanathan A, Patil V, Arora A, Hegde AS, Arivazhagan A, Santosh V and Somasundaram K. Essential role of METTL3-mediated m(6)A modification in glioma stem-like cells maintenance and radioresistance. Oncogene 2018; 37: 522-533.
[28] Lin S, Choe J, Du P, Triboulet R and Gregory RI. The m(6)A methyltransferase METTL3 promotes translation in human cancer cells. Mol Cell 2016; 62: 335-345.
[29] Wang K, Jiang L, Zhang Y and Chen C. Progression of thyroid carcinoma is promoted by the m6A methyltransferase METTL3 through regulating m(6)A methylation on TCF1. Onco Targets Ther 2020; 13: 1605-1612.
[30] Wang X, Fu X, Zhang J, Xiong C, Zhang S and Lv Y. Identification and validation of m(6)A RNA methylation regulators with clinical prognostic value in Papillary thyroid cancer. Cancer Cell Int 2020; 20: 203.
[31] Wang YL, Feng SH, Guo SC, Wei WJ, Li DS, Wang Y, Wang X, Wang ZY, Ma YY, Jin L, Ji QH and Wang JC. Confirmation of papillary thyroid cancer susceptibility loci identified by genome-wide association studies of chromosomes 14q13, 9q22, 2q35 and 8p12 in a Chinese population. J Med Genet 2013; 50: 689-695.
[32] Matsuse M, Takahashi M, Mitsutake N, Nishihara E, Hirokawa M, Kawaguchi T, Rogounovitch T, Saenko V, Bychkov A, Suzuki K, Matsuo K, Tajima K, Miyauchi A, Yamada R, Matsuda F and Yamashita S. The FOXE1 and NKX2-1 loci are associated with susceptibility to papillary thyroid carcinoma in the Japanese population. J Med Genet 2011; 48: 645-648.
[33] Liyanarachchi S, Wojcicka A, Li W, Czetwertynska M, Stachlewska E, Nagy R, Hoag K, Wen B, Ploski R, Ringel MD, Kozłowicz-Gudzinska I, Gierlikowski W, Jazdzewski K, He H and de la Chapelle A. Cumulative risk impact of five genetic variants associated with papillary thyroid carcinoma. Thyroid 2013; 23: 1532-1540.
[34] Jones AM, Howarth KM, Martin L, Gorman M, Mihai R, Moss L, Auton A, Lemon C, Mehanna H, Mohan H, Clarke SE, Wadsley J, Macias E, Coatesworth A, Beasley M, Roques T, Martin C, Ryan P, Gerrard G, Power D, Bremmer C; TCUKIN Consortium, Tomlinson I and Carvajal-

Carmona LG. Thyroid cancer susceptibility polymorphisms: confirmation of loci on chromosomes 9q22 and 14q13, validation of a recessive 8q24 locus and failure to replicate a locus on 5q24. J Med Genet 2012; 49: 158-163.

[35] Zheng Y, Nie P, Peng D, He Z, Liu M, Xie Y, Miao Y, Zuo Z and Ren J. m6AVar: a database of functional variants involved in m6A modification. Nucleic Acids Res 2018; 46: D139-d145.

[36] Zhou W, Nielsen JB, Fritsche LG, Dey R, Gabrielsen ME, Wolford BN, LeFaive J, VandeHaar P, Gagliano SA, Gifford A, Bastarache LA, Wei WQ, Denny JC, Lin M, Hveem K, Kang HM, Abecasis GR, Willer CJ and Lee S. Efficiently controlling for case-control imbalance and sample relatedness in large-scale genetic association studies. Nat Genet 2018; 50: 1335-1341.

[37] Gudmundsson J, Thorleifsson G, Sigurdsson JK, Stefansdottir L, Jonasson JG, Gudjonsson SA, Gudbjartsson DF, Masson G, Johannsdottir H, Halldorsson GH, Stacey SN, Helgason H, Sulem P, Senter L, He H, Liyanarachchi S, Ringel MD, Aguillo E, Panadero A, Prats E, Garcia-Castaño A, De Juan A, Rivera F, Xu L, Kiemeney LA, Eyjolfsson GI, Sigurdardottir O, Olafsson I, Kristvinsson H, Netea-Maier RT, Jonsson T, Mayordomo JI, Plantinga TS, Hjartarson H, Hrafnkelsson J, Sturgis EM, Thorsteinsdottir U, Rafnar T, de la Chapelle A and Stefansson K. A genome-wide association study yields five novel thyroid cancer risk loci. Nat Commun 2017; 8: 14517.

[38] Anders S, Pyl PT and Huber W. HTSeq--a Python framework to work with high-throughput sequencing data. Bioinformatics 2015; 31: 166-169.

[39] Li Z, Weng H, Su R, Weng X, Zuo Z, Li C, Huang H, Nachtergaele S, Dong L, Hu C, Qin X, Tang L, Wang Y, Hong GM, Huang H, Wang X, Chen P, Gurbuxani S, Arnovitz S, Li Y, Li S, Strong J, Neilly MB, Larson RA, Jiang X, Zhang P, Jin J, He C and Chen J. FTO plays an oncogenic role in acute myeloid leukemia as a N(6)-methyladenosine RNA demethylase. Cancer Cell 2017; 31: 127-141.

[40] Wang X, Lu Z, Gomez A, Hon GC, Yue Y, Han D, Fu Y, Parisien M, Dai Q, Jia G, Ren B, Pan T and He C. N6-methyladenosine-dependent regulation of messenger RNA stability. Nature 2014; 505: 117-120.

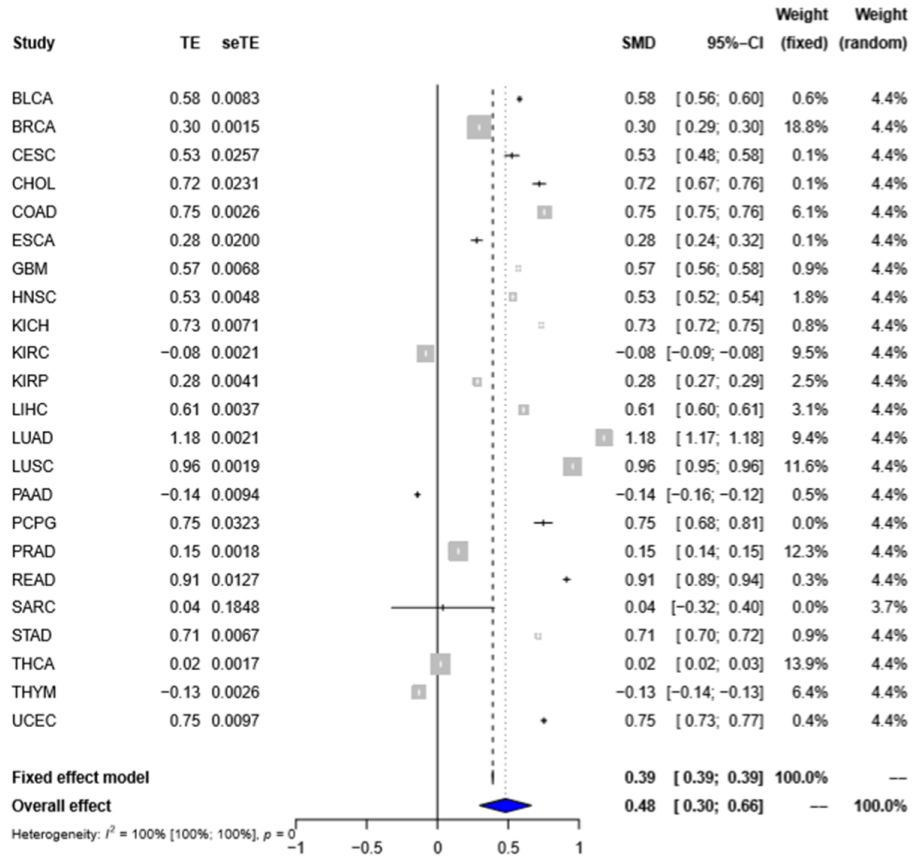
Study TE seTE SMD 95%−CI Weight (fixed) Weight (random)
BLCA 0.58 0.0083 0.58 [0.56; 0.60] 0.6% 4.4%
BRCA 0.30 0.0015 0.30 [0.29; 0.30] 18.8% 4.4%
CESC 0.53 0.0257 0.53 [0.48; 0.58] 0.1% 4.4%
CHOL 0.72 0.0231 0.72 [0.67; 0.76] 0.1% 4.4%
COAD 0.75 0.0026 0.75 [0.75; 0.76] 6.1% 4.4%
ESCA 0.28 0.0200 0.28 [0.24; 0.32] 0.1% 4.4%
GBM 0.57 0.0068 0.57 [0.56; 0.58] 0.9% 4.4%
HNSC 0.53 0.0048 0.53 [0.52; 0.54] 1.8% 4.4%
KICH 0.73 0.0071 0.73 [0.72; 0.75] 0.8% 4.4%
KIRC −0.08 0.0021 −0.08 [−0.09; −0.08] 9.5% 4.4%
KIRP 0.28 0.0041 0.28 [0.27; 0.29] 2.5% 4.4%
LIHC 0.61 0.0037 0.61 [0.60; 0.61] 3.1% 4.4%
LUAD 1.18 0.0021 1.18 [1.17; 1.18] 9.4% 4.4%
LUSC 0.96 0.0019 0.96 [0.95; 0.96] 11.6% 4.4%
PAAD −0.14 0.0094 −0.14 [−0.16; −0.12] 0.5% 4.4%
PCPG 0.75 0.0323 0.75 [0.68; 0.81] 0.0% 4.4%
PRAD 0.15 0.0018 0.15 [0.14; 0.15] 12.3% 4.4%
READ 0.91 0.0127 0.91 [0.89; 0.94] 0.3% 4.4%
SARC 0.04 0.1848 0.04 [−0.32; 0.40] 0.0% 3.7%
STAD 0.71 0.0067 0.71 [0.70; 0.72] 0.9% 4.4%
THCA 0.02 0.0017 0.02 [0.02; 0.03] 13.9% 4.4%
THYM −0.13 0.0026 −0.13 [−0.14; −0.13] 6.4% 4.4%
UCEC 0.75 0.0097 0.75 [0.73; 0.77] 0.4% 4.4%
Fixed effect model 0.39 [0.39; 0.39] 100.0% –
Overall effect 0.48 [0.30; 0.66] – 100.0%
Heterogeneity: I^2 = 100% [100%; 100%], p = 0
−1 −0.5 0 0.5 1

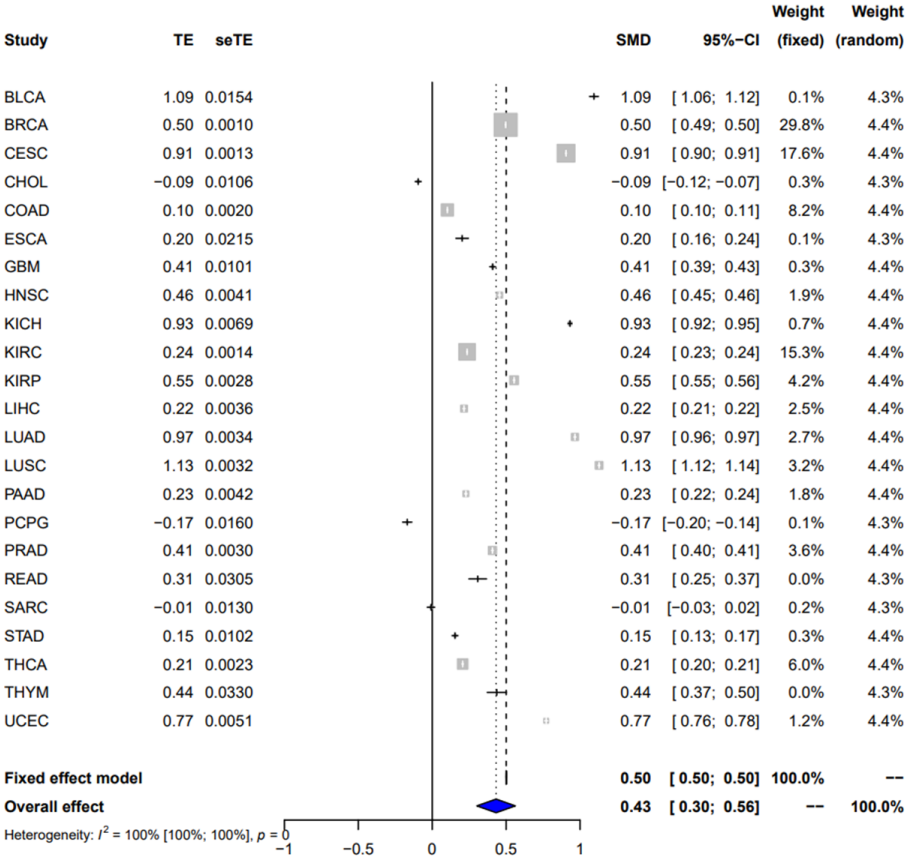
Study TE seTE SMD 95%−CI Weight (fixed) Weight (random)
BLCA 1.09 0.0154 1.09 [1.06; 1.12] 0.1% 4.3%
BRCA 0.50 0.0010 0.50 [0.49; 0.50] 29.8% 4.4%
CESC 0.91 0.0013 0.91 [0.90; 0.91] 17.6% 4.4%
CHOL −0.09 0.0106 −0.09 [−0.12; −0.07] 0.3% 4.3%
COAD 0.10 0.0020 0.10 [0.10; 0.11] 8.2% 4.4%
ESCA 0.20 0.0215 0.20 [0.16; 0.24] 0.1% 4.3%
GBM 0.41 0.0101 0.41 [0.39; 0.43] 0.3% 4.4%
HNSC 0.46 0.0041 0.46 [0.45; 0.46] 1.9% 4.4%
KICH 0.93 0.0069 0.93 [0.92; 0.95] 0.7% 4.4%
KIRC 0.24 0.0014 0.24 [0.23; 0.24] 15.3% 4.4%
KIRP 0.55 0.0028 0.55 [0.55; 0.56] 4.2% 4.4%
LIHC 0.22 0.0036 0.22 [0.21; 0.22] 2.5% 4.4%
LUAD 0.97 0.0034 0.97 [0.96; 0.97] 2.7% 4.4%
LUSC 1.13 0.0032 1.13 [1.12; 1.14] 3.2% 4.4%
PAAD 0.23 0.0042 0.23 [0.22; 0.24] 1.8% 4.4%
PCPG −0.17 0.0160 −0.17 [−0.20; −0.14] 0.1% 4.3%
PRAD 0.41 0.0030 0.41 [0.40; 0.41] 3.6% 4.4%
READ 0.31 0.0305 0.31 [0.25; 0.37] 0.0% 4.3%
SARC −0.01 0.0130 −0.01 [−0.03; 0.02] 0.2% 4.3%
STAD 0.15 0.0102 0.15 [0.13; 0.17] 0.3% 4.4%
THCA 0.21 0.0023 0.21 [0.20; 0.21] 6.0% 4.4%
THYM 0.44 0.0330 0.44 [0.37; 0.50] 0.0% 4.3%
UCEC 0.77 0.0051 0.77 [0.76; 0.78] 1.2% 4.4%
Fixed effect model 0.50 [0.50; 0.50] 100.0% –
Overall effect 0.43 [0.30; 0.56] – 100.0%
Heterogeneity: I^2 = 100% [100%; 100%], p = 0
−1 −0.5 0 0.5 1

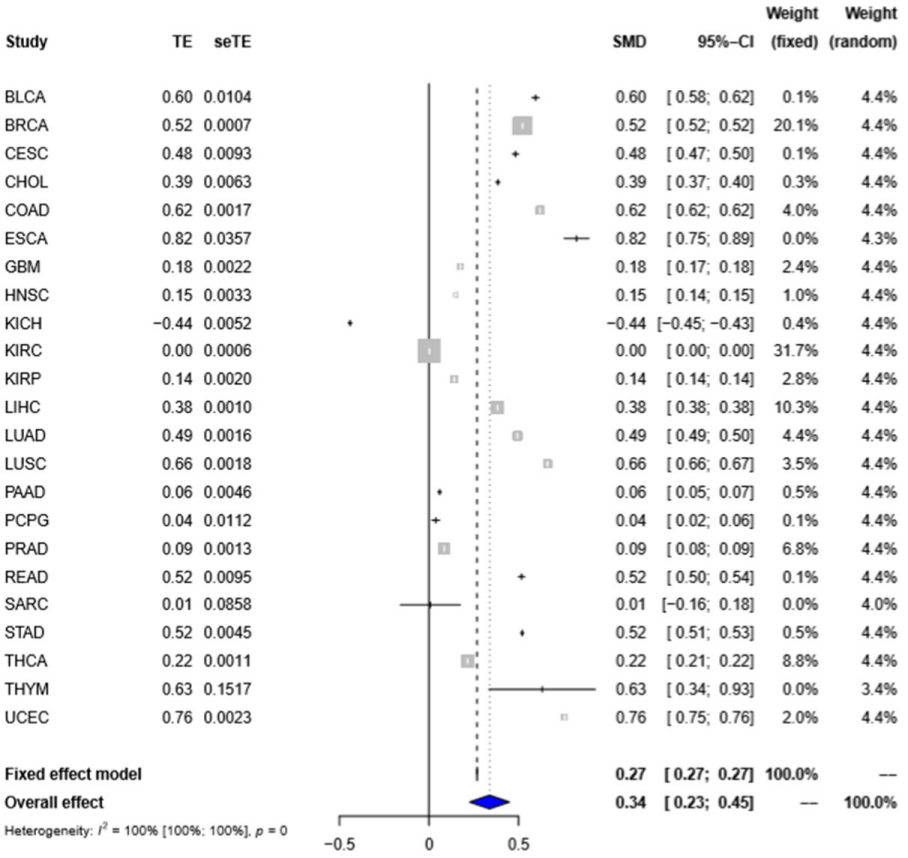
Study TE seTE SMD 95%−CI Weight (fixed) Weight (random)
BLCA 0.60 0.0104 0.60 [0.58; 0.62] 0.1% 4.4%
BRCA 0.52 0.0007 0.52 [0.52; 0.52] 20.1% 4.4%
CESC 0.48 0.0093 0.48 [0.47; 0.50] 0.1% 4.4%
CHOL 0.39 0.0063 0.39 [0.37; 0.40] 0.3% 4.4%
COAD 0.62 0.0017 0.62 [0.62; 0.62] 4.0% 4.4%
ESCA 0.82 0.0357 0.82 [0.75; 0.89] 0.0% 4.3%
GBM 0.18 0.0022 0.18 [0.17; 0.18] 2.4% 4.4%
HNSC 0.15 0.0033 0.15 [0.14; 0.15] 1.0% 4.4%
KICH −0.44 0.0052 −0.44 [−0.45; −0.43] 0.4% 4.4%
KIRC 0.00 0.0006 0.00 [0.00; 0.00] 31.7% 4.4%
KIRP 0.14 0.0020 0.14 [0.14; 0.14] 2.8% 4.4%
LIHC 0.38 0.0010 0.38 [0.38; 0.38] 10.3% 4.4%
LUAD 0.49 0.0016 0.49 [0.49; 0.50] 4.4% 4.4%
LUSC 0.66 0.0018 0.66 [0.66; 0.67] 3.5% 4.4%
PAAD 0.06 0.0046 0.06 [0.05; 0.07] 0.5% 4.4%
PCPG 0.04 0.0112 0.04 [0.02; 0.06] 0.1% 4.4%
PRAD 0.09 0.0013 0.09 [0.08; 0.09] 6.8% 4.4%
READ 0.52 0.0095 0.52 [0.50; 0.54] 0.1% 4.4%
SARC 0.01 0.0858 0.01 [−0.16; 0.18] 0.0% 4.0%
STAD 0.52 0.0045 0.52 [0.51; 0.53] 0.5% 4.4%
THCA 0.22 0.0011 0.22 [0.21; 0.22] 8.8% 4.4%
THYM 0.63 0.1517 0.63 [0.34; 0.93] 0.0% 3.4%
UCEC 0.76 0.0023 0.76 [0.75; 0.76] 2.0% 4.4%
Fixed effect model 0.27 [0.27; 0.27] 100.0% —
Overall effect 0.34 [0.23; 0.45] — 100.0%
Heterogeneity: I^2 = 100% [100%; 100%], p = 0
−0.5 0 0.5

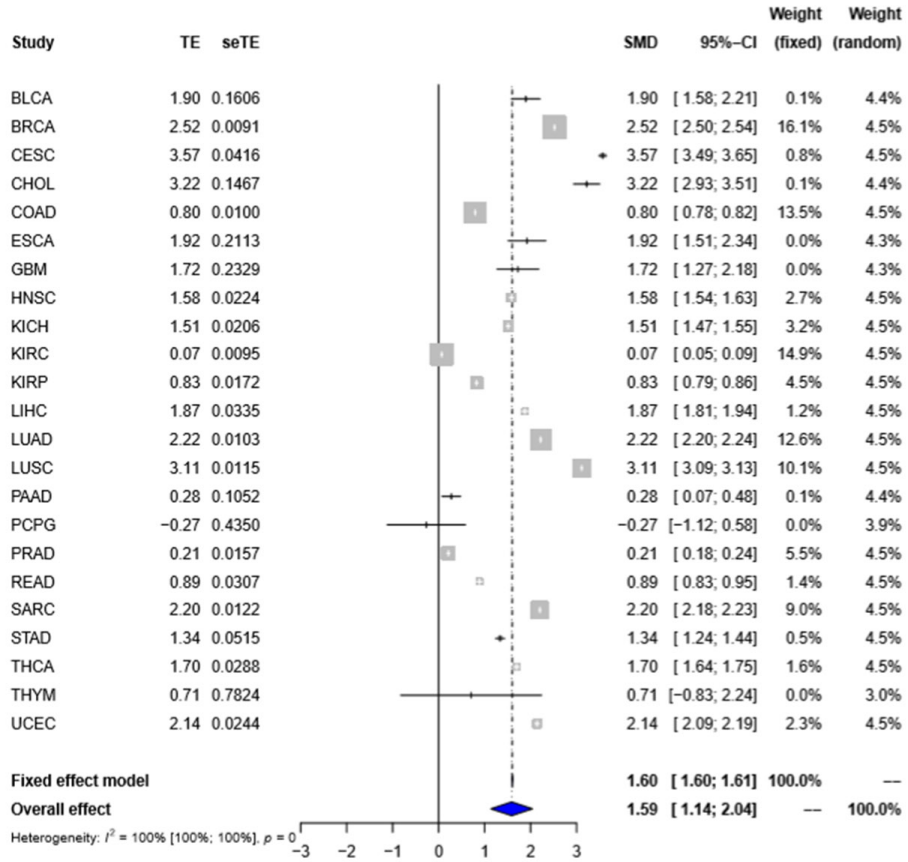
Study TE seTE SMD 95%−CI Weight (fixed) Weight (random)
BLCA 1.90 0.1606 1.90 [1.58; 2.21] 0.1% 4.4%
BRCA 2.52 0.0091 2.52 [2.50; 2.54] 16.1% 4.5%
CESC 3.57 0.0416 3.57 [3.49; 3.65] 0.8% 4.5%
CHOL 3.22 0.1467 3.22 [2.93; 3.51] 0.1% 4.4%
COAD 0.80 0.0100 0.80 [0.78; 0.82] 13.5% 4.5%
ESCA 1.92 0.2113 1.92 [1.51; 2.34] 0.0% 4.3%
GBM 1.72 0.2329 1.72 [1.27; 2.18] 0.0% 4.3%
HNSC 1.58 0.0224 1.58 [1.54; 1.63] 2.7% 4.5%
KICH 1.51 0.0206 1.51 [1.47; 1.55] 3.2% 4.5%
KIRC 0.07 0.0095 0.07 [0.05; 0.09] 14.9% 4.5%
KIRP 0.83 0.0172 0.83 [0.79; 0.86] 4.5% 4.5%
LIHC 1.87 0.0335 1.87 [1.81; 1.94] 1.2% 4.5%
LUAD 2.22 0.0103 2.22 [2.20; 2.24] 12.6% 4.5%
LUSC 3.11 0.0115 3.11 [3.09; 3.13] 10.1% 4.5%
PAAD 0.28 0.1052 0.28 [0.07; 0.48] 0.1% 4.4%
PCPG −0.27 0.4350 −0.27 [−1.12; 0.58] 0.0% 3.9%
PRAD 0.21 0.0157 0.21 [0.18; 0.24] 5.5% 4.5%
READ 0.89 0.0307 0.89 [0.83; 0.95] 1.4% 4.5%
SARC 2.20 0.0122 2.20 [2.18; 2.23] 9.0% 4.5%
STAD 1.34 0.0515 1.34 [1.24; 1.44] 0.5% 4.5%
THCA 1.70 0.0288 1.70 [1.64; 1.75] 1.6% 4.5%
THYM 0.71 0.7824 0.71 [−0.83; 2.24] 0.0% 3.0%
UCEC 2.14 0.0244 2.14 [2.09; 2.19] 2.3% 4.5%
Fixed effect model 1.60 [1.60; 1.61] 100.0% —
Overall effect 1.59 [1.14; 2.04] — 100.0%
Heterogeneity: I^2 = 100% [100%; 100%], p = 0
−3 −2 −1 0 1 2 3

Supplementary Figure 1. Pan-cancer up-regulation of PLEKHA8, SMUG1, CDC123 and RMI2 cross 23 types of human cancers. Cancer samples were collected from the TCGA project (N = 10,490). Gene expression level was log2 transformed before the meta-analysis. Both fixed effect model and random effect model were applied for the aggregation. 95% CI was applied to show the risk and protective effect to overall survival time. In order to show more details for different studies, any standardized mean difference (SMD) higher than 3 and lower than -3 was showed with arrow. Blue filled parallelograms represent the SMD for fixed effect model and random effect model.

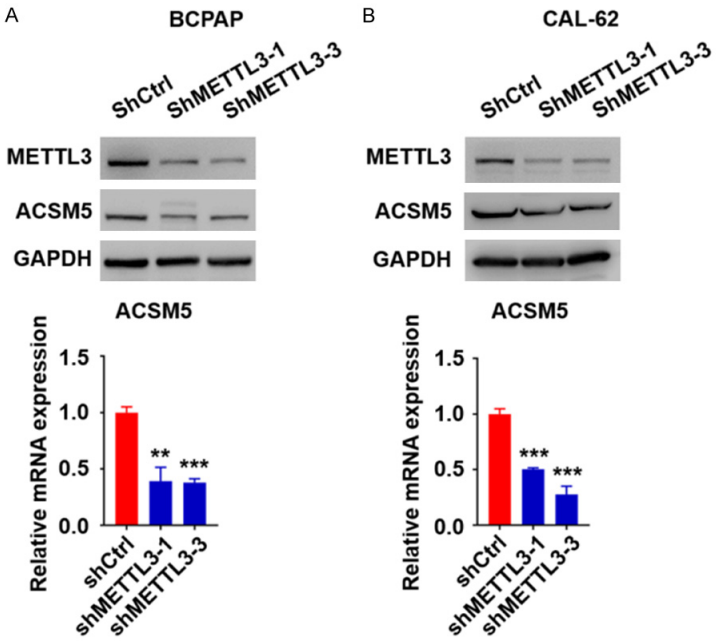

Supplementary Figure 2. ACSM5 was downregulated in METTL3 knowdown stable cell. A. ACSM5 mRNA and protein expression levels were stably knocked down METTL3 in BCPAP cells. B. ACSM5 mRNA and protein expression levels were stably knocked down METTL3 in Cal-62 cells.

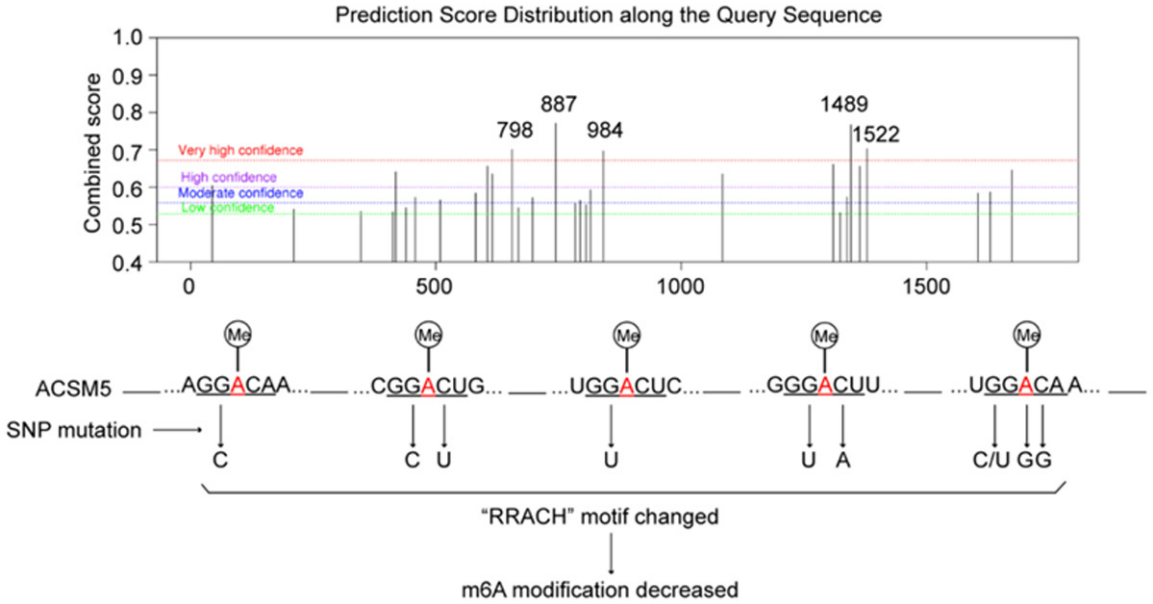

Supplementary Figure 3. SNP mutations at the m6A modification sites of ACSM5 mRNA. SRAMP (http://www.cuilab.cn/sramp) was used to predict the m6A modification site of ACSM5. We selected five very high confidence modification sites to overlap with the SNP sites in PubMed (https://www.ncbi.nlm.nih.gov/), and finally found all the very high confidence m6A modification sites contain SNPs.

Supplementary Table 1. Thyroid cancer associated SNPs

SNP	Chromosome	Position	P	Symbol
ENSG00000175643	16	11343475	3.90E-14	RMI2
ENSG00000106367	7	100797677	3.61E-12	AP1S1
ENSG00000106086	7	30068040	8.36E-10	PLEKHA8
ENSG00000183549	16	20420855	4.74E-09	ACSM5
ENSG00000123415	12	54558528	2.34E-08	SMUG1
ENSG00000198663	6	36839645	4.33E-08	C6orf89
ENSG00000151465	10	12237963	1.52E-07	CDC123
ENSG00000204267	6	32789609	1.69E-07	TAP2
ENSG00000062725	17	58520519	3.11E-06	APPBP2
ENSG00000197619	19	52494584	3.21E-06	ZNF615
ENSG00000158022	1	26377794	9.20E-06	TRIM63
ENSG00000141580	17	80572437	1.00E-05	WDR45B
ENSG00000151553	10	116581502	1.06E-05	FAM160B1
ENSG00000122729	9	32384617	2.36E-05	ACO1
ENSG00000143437	1	150782180	7.72E-05	ARNT
ENSG00000141012	16	88880141	0.000127038	GALNS
ENSG00000106733	9	77675488	0.000186512	NMRK1
ENSG00000132793	20	39969559	0.00027026	LPIN3
ENSG00000152223	18	43427573	0.000302933	EPG5
ENSG00000104626	8	8869172	0.001127183	ERI1
ENSG00000081692	1	227918125	0.001299691	JMJD4
ENSG00000172014	9	69381811	0.001846155	ANKRD20A4
ENSG00000163945	4	1341053	0.002209206	UVSSA
ENSG00000151498	11	134123388	0.004290753	ACAD8
ENSG00000112294	6	24495079	0.006027414	ALDH5A1
ENSG00000160703	11	119037276	0.009695353	NLRX1
ENSG00000182195	23	140269933	0.014234074	LDOC1
ENSG00000142794	1	21766620	0.01870655	NBPF3
ENSG00000134253	1	117653681	0.020108862	TRIM45
ENSG00000110218	11	93862093	0.020231489	PANX1
ENSG00000196418	1	247285276	0.023276776	ZNF124
ENSG00000167526	16	89627064	0.027260647	RPL13
ENSG00000152133	2	37311593	0.038865209	GPATCH11
ENSG00000143622	1	155867598	0.049230287	RIT1
ENSG00000175137	1	249104647	0.053215216	SH3BP5L
ENSG00000272047	6	158589383	0.056786339	GTF2H5
ENSG00000258986	14	104941014	0.057156298	TMEM179
ENSG00000189339	1	1592938	0.068973477	SLC35E2B
ENSG00000185344	12	124196864	0.082654907	ATP6V0A2
ENSG00000108556	17	4801068	0.09321947	CHRNE
ENSG00000026652	6	161551010	0.104240303	AGPAT4
ENSG00000188549	15	40625957	0.117766531	C15orf52
ENSG00000122863	10	73724122	0.118504258	CHST3
ENSG00000137815	15	41700605	0.122108612	RTF1
ENSG00000099974	22	24309088	0.123741862	DDTL
ENSG00000105866	7	21467651	0.134214203	SP4
ENSG00000173875	19	12721731	0.139149896	ZNF791

ENSG00000154328	8	11627147	0.173379789	NEIL2
ENSG00000144120	2	120436742	0.180867102	TMEM177
ENSG00000071794	3	148747913	0.186128117	HLTF
ENSG00000134987	5	110427413	0.199473721	WDR36
ENSG00000111652	12	6832906	0.21393205	COPS7A
ENSG00000080345	2	152266396	0.21881116	RIF1
ENSG00000146530	7	12370510	0.231395382	VWDE
ENSG00000063587	23	152599612	0.245814683	ZNF275
ENSG00000186470	6	26365386	0.281587984	BTN3A2
ENSG00000133731	8	82570195	0.301570374	IMPA1
ENSG00000009950	7	73007523	0.338022053	MLXIPL
ENSG00000136720	2	128994289	0.339160585	HS6ST1
ENSG00000166454	16	81069451	0.370903022	ATMIN
ENSG00000186716	22	23521890	0.375526758	BCR
ENSG00000185100	14	105190522	0.418810204	ADSSL1
ENSG00000149639	20	35405844	0.463213652	SOGA1
ENSG00000160305	21	47878811	0.470488471	DIP2A
ENSG00000139433	12	110288747	0.534014739	GLTP
ENSG00000179344	6	32627243	0.563739971	HLA-DQB1
ENSG00000196683	7	22852250	0.574919996	TOMM7
ENSG00000165629	10	7830091	0.603768381	ATP5C1
ENSG00000117228	1	89518001	0.632524545	GBP1
ENSG00000171435	12	117890816	0.651713468	KSR2
ENSG00000171903	19	16023176	0.660140474	CYP4F11
ENSG00000198231	17	61850962	0.671194476	DDX42
ENSG00000130770	1	28562619	0.756479013	ATPIF1
ENSG00000108064	10	60144781	0.775560214	TFAM
ENSG00000113812	3	53901092	0.776173575	ACTR8
ENSG00000153786	16	85007786	0.82856826	ZDHHC7
ENSG00000116260	1	180123968	0.850991728	QSOX1
ENSG00000166037	11	95523128	0.918192862	CEP57
ENSG00000105419	19	47906380	0.961025221	MEIS3
ENSG00000105750	19	21106027	0.963100186	ZNF85

Supplementary Table 2. The clinical pathological characteristics of the patients involved

Number	Gender	Age	Pathological type	T stage	N stage	M stage	AJCC stage
1	Male	8	PTC	3	1b	0	1
2	Female	69	PTC	3b	0	0	2
3	Male	41	PTC	1	0	0	1
4	Female	42	PTC	1a	1a	0	1
5	Female	26	PTC	1a	1a	0	1
6	Female	49	PTC	1	0	0	1
7	Female	28	PTC	4a	1b	0	1
8	Male	38	PTC	1a	1a	0	1
9	Female	25	PTC	1b	1b	0	1
10	Female	52	PTC	3b	1a	0	1
11	Female	47	PTC	1	1a	0	1
12	Male	43	PTC	1a	0	0	1
13	Female	47	PTC	1b	1a	0	1
14	Male	50	PTC	1a	0	0	1
15	Female	42	PTC	1b	1a	0	1
16	Male	19	PTC	2	1b	0	1

Supplementary Table 3. Primers Sequence (5’ to 3’)

CDC123 Former primer	GATGGAACTCTGGTGGTTTCAGG
CDC123 Reverse primer	CTTCCTGGACTTTAGTGSMUG1GCAAAC
SMUG1 Former primer	CTTCCTGGACTTTAGTGGCAAAC
SMUG1 Reverse primer	CTGGTCGTTTAGGATGCTCTTGG
PLEKHA8 Former primer	GGGAGCATACAAATGGCAGTCTG
PLEKHA8 Reverse primer	CCGCTGTCTTTCAGCCACACTT
ACSM5 Former primer	CCATCTTTCGGCTGCTTGTGCA
ACSM5 Reverse primer	CAGTCTGGTGTTTCCACTTCTCC
RMI2 Former primer	ACTTCATAACTTTCGGCGAGAC
RMI2 Reverse primer	CAGACAGCAGAAACCCAACATT
β-Actin Former primer	GATCATTGCTCCTCCTGAGC
β-Actin Reverse primer	ACTCCTGCTTGCTGATCCAC